



Stress-corrosion mechanisms in silicate glasses

Matteo Ciccotti

► To cite this version:

| Matteo Ciccotti. Stress-corrosion mechanisms in silicate glasses. 2008. hal-00354121v1

HAL Id: hal-00354121

<https://hal.science/hal-00354121v1>

Preprint submitted on 19 Jan 2009 (v1), last revised 1 Apr 2009 (v2)

HAL is a multi-disciplinary open access archive for the deposit and dissemination of scientific research documents, whether they are published or not. The documents may come from teaching and research institutions in France or abroad, or from public or private research centers.

L'archive ouverte pluridisciplinaire **HAL**, est destinée au dépôt et à la diffusion de documents scientifiques de niveau recherche, publiés ou non, émanant des établissements d'enseignement et de recherche français ou étrangers, des laboratoires publics ou privés.

REVIEW ARTICLE

Stress-corrosion mechanisms in silicate glasses

Matteo Ciccotti

Laboratoire des Colloïdes, Verres et Nanomatériaux, UMR 5587, CNRS, Université Montpellier 2, Montpellier, France

E-mail: `matteo.ciccotti@univ-montp2.fr`

Abstract. The present review is intended to revisit the advances and debates in the comprehension of the mechanisms of subcritical crack propagation in silicate glasses after almost a century of its initial developments. Glass has inspired the initial insights of Griffith on the origin of brittleness and the following development of modern fracture mechanics. Yet, through the decades the real nature of the fundamental mechanisms of crack propagation in glass has escaped a clear comprehension that may gather general agreement on subtle problems such as the role of plasticity, the role of the glass composition, the environmental condition at the crack tip and its relation with the complex mechanisms of corrosion and leaching. The different processes are analysed here with a special focus on their relevant space and time scales in order to question their domain of action and their contribution in both the kinetics laws and the energetic aspects.

Submitted to: *J. Phys. D: Appl. Phys.*

<i>CONTENTS</i>	2
Contents	
1 Introduction	3
2 Space and time scales of fracture mechanics	5
3 Crack propagation kinetics	9
3.1 Zone I: stress-corrosion regime	10
3.2 Zone II: transport limited propagation	12
3.3 Zone III: inert propagation and failure	13
3.4 Zone 0: threshold behaviour, healing and aging	14
4 A deeper insight in the stress-corrosion and damage mechanisms	16
4.1 Competition between dissolution, corrosion and leaching	16
4.2 Crack tip blunting	18
4.3 Crack tip plasticity	20
4.4 Local crack tip environment	24
4.5 Alkali ion migration under stress gradient	26
4.6 Fracture surfaces	28
5 Perspectives	29

1. Introduction

Silicate glasses are highly homogeneous and isotropic materials at scales larger than a few nanometers, thus making continuum descriptions well suited down to submicrometric scales. This strong degree of homogeneity is at the origin of the best glass properties, such as the elevated degree of transparency, but it is also partly the cause of a major limitation: brittleness! Glass products break very easily when subjected to even weak impacts with hard materials, and also the static stress that can be sustained by a glass product for a convenient time without fracturing is quite low (Gy 2003). The extreme homogeneity of glass along with the elevated strength of its covalent cohesive bonds cause a huge stress concentration in a nanometric region around small defects. The local evolution of damage is thus very efficient, involving very little bulk dissipation and relatively efficient conversion of the mechanical energy into the surface energy required to create new fracture surfaces.

The earliest works of Griffith (1921) have identified the origin of the low strength of glass in the unavoidable presence of small flaws in glass objects. These flaws are generally interpreted as submicrometric surface cracks that escape to optical inspection. Worse than this, these stress concentrators are responsible of a local acceleration of the corrosive interaction of glass by the environment. The damage will then generally spread in time even under moderate global stresses, leading eventually to a delayed failure, especially in the presence of a moist atmosphere. This phenomenon, named static fatigue, is generally interpreted as the combination of an initial stage of differential stress-enhanced corrosion (Charles et Hillig 1962) leading to the progressive sharpening of the flaws until the crack tip radius reaches a molecular (nanometric) dimension, and a second stage of stationary slow crack growth (Wiederhorn and Bolz 1970) with the stress-corrosion reactions concentrated at the molecularly sharp crack tip.

The development of fracture mechanics has allowed to rationalise the fracture resistance of glass by describing the conditions of propagation of a single major fracture in a glass sample. The earliest introduction by Griffith of the strain energy release rate G , and then of the stress intensity factor K (Irwin and Washington 1957) have allowed to determine a more fundamental fracture criterion and more robustly defined fracture parameters for crack propagation in the form of critical values G_c or K_c . Yet, in most practical cases G_c can be quite larger than twice the equilibrium surface energy of the material, implying the occurrence of other subsidiary dissipation mechanisms in the fracture process.

The brittleness of glass can thus be read as the elevated efficiency of conversion of elastic energy into surface energy, suggesting a very weak contribution of plastic deformation and other bulk dissipation mechanisms, which would involve at most a region of few nanometers around the crack tip. The values of K_c for most glasses are of the order of $1 \text{ MPam}^{1/2}$, which is rather low, especially when compared to the 50 fold larger values in metals where the energy dissipation by bulk ductility is dominant in the fracture energy.

In the fracture mechanics framework the subcritical propagation by stress-corrosion can be well rationalised and represented as a $v(K)$ or $G(v)$ relation for $K < K_c$ (Wiederhorn and Bolz 1970). This was shown to generally involve three propagation regions as shown by Wiederhorn (c.f. Fig. 4). Region I corresponds to the cited stress-corrosion regime, where the crack propagates due to a stress-enhanced corrosion reaction, which is strongly dependent on the environment. In region II the propagation velocity is limited by the transport kinetics of environmental corrosive molecules to the crack tip. In region III the stresses are strong enough to induce the bond breaking in the absence of corrosion reactions, the velocity rises very sharply with K eventually reaching the critical propagation at K_c . For some glass compositions, a threshold behaviour appears for $K = K_0$ leading to what is generally called region 0 (Michalske 1977).

Phenomenological equations such as Wiederhorn's can describe the dependence of crack velocity on stress and on environmental parameters for most typical glasses and are compatible with a thorough consistent modelling based on the sharp-crack atomic-bonding paradigm (Lawn 1993). Yet the detailed nature of the stress-corrosion mechanisms that occur at the crack tip have been debated for decades (Marsh 1964b; Maugis 1985; Gehrke *et al* 1991; Tomozawa 1996), and a general disagreement can be found on the relevance of several accessory phenomena that may participate in the stress-corrosion mechanisms at different stages of the process. Stress-corrosion can involve a complex interplay between the diffusion of reactive molecules (mainly water) into the crack cavity and into the glass network, the corrosion (or dissolution) of the network itself, and the migration of weakly bonded alkali ions under chemical or stress gradient (Gehrke *et al* 1991; Bunker 1994). All these phenomena are typically very slow at ambient conditions in the unstressed material, but they can significantly accelerate in the highly stressed neighbourhood of the crack tip, depending especially on the nature of the environment and of its confinement. Their time scales will be progressively accelerated in a series of smaller and smaller shells of increasing stress when approaching the crack tip. However, since the crack tip is propagating, the different phenomena will be able to spread or not in each shell depending on a competition between their time scale in each shell and the crack propagation velocity. Since the size of the activated shells can vary from microns to nanometers depending on the interplay between space and time scales, the modelling of these phenomena requires nanometer scale resolved investigation techniques and questioning about the relevant physical laws at the nanoscale. Such investigation is very promising in order to solve the debates by direct observation and to relate the phenomenological parameters to the specific composition and structure of glasses.

The development of several nanoscale investigation techniques in the 80's has allowed significant insight in the comprehension of the different mechanisms. In particular SEM, TEM and AFM measurements of both *post-mortem* crack surfaces and direct *in-situ* observations of the crack tip neighbourhood have permitted the investigation of the space and time scales of occurrence of these phenomena under specific conditions (c.f. section 4.3). The progressive decrease in resolution down to the

micron scale of several structural and compositional analysis techniques (such as Raman, IR, Brillouin spectroscopies, X-Ray, electron and Neutron scattering, NMR, XPS, SIMS) have also permitted to investigate the alterations of the bulk glass near the crack tip or at freshly fractured surfaces (c.f. section 4.6). These techniques, combined with the increasing power of molecular and quantum dynamics simulations are permitting great insights in the understanding of the combination between mechanical and chemical processes acting at the crack tip.

Section 2 will first focus on some relevant concepts of fracture mechanics. In section 3 the most solidly established features of the slow crack propagation kinetics in glasses will be described and interpreted in the framework of the classic sharp-crack atomic-bonding paradigm proposed in the '70s. The section 4 of the review will present a deeper discussion of the relations between the crack propagation and the chemical mechanisms of stress-corrosion, along with a critical analysis of the points which are still controversial and of the recent experimental evidences and efforts which have been done to make them more clear. A concluding section will discuss the perspectives and promises of the development of this interesting research field.

2. Space and time scales of fracture mechanics

The world of fracture mechanics is extremely wide and rich of theories and variants that account the many peculiar manifestations in different materials. It is difficult to figure out the 'one theory' that can encompass different phenomena such as atomic bond breaking, dislocation motion, viscoelastic-plastic flow, damage spreading, corrosion, ion exchange, cavitation, fingering and a whole plethora of other fancy effects. Different application communities generally end up with following different paths, along with different terms, variables and philosophies. Luckily enough, the classic Linear Elastic Fracture Mechanics (LEFM) was mainly developed to tackle strength problems of brittle materials like glass, which constitutes a privileged material for its understanding and application. While inviting the reader to the very comprehensive book of Lawn (1993) on the fracture of brittle solids, I will recall here the concepts which are relevant to follow the point of view of the present review and the discussed issues.

Although the ideal basic mechanism for fracture is the conversion of mechanical energy into surface energy (Griffith 1921), fracture propagation is generally complicated by the activation of subsidiary dissipation mechanisms that generally act in a bulk neighbourhood of the crack tip called the process zone (Irwin 1960), but who can also extend to the whole material volume or act between the open crack walls as illustrated in the schematical model in Fig. 1. The energy dissipated by each of these mechanisms has to be taken into account to estimate the energy that is necessary to propagate fracture by a unit area. To progressively account for nonlinear effects, irreversibility and dissipative processes, fracture mechanics has undergone several profound developments, which however were managed with appreciable devotion in order to preserve the formalism of LEFM (Orowan 1955; Irwin 1960; Barenblatt 1962; Rice 1968; Rice 1978; Lawn

1993). This is based on one side on the use of surface energy balance related variables such as the strain energy release rate G (Griffith 1921) and on the other on variables describing the fundamental inverse square root dependence of the stress field on the crack tip distance such as the stress intensity factor K (Irwin and Washington 1957)‡. Moreover, the two kinds of variable remain in general related by an equivalence in the typical form $G = K^2/E'$ (E' being an equivalent Young modulus) and the criteria for equilibrium and crack propagation can still generally be expressed by equations of the kind $G \geq G_c$ or $K \geq K_c$ by only changing the exact meaning of the variables used (Lawn 1993).

For what concerns the description of the kinetics of fracture, we can distinguish between two main different approaches: the ones where the dissipated energy dominates on the surface energy and the ones where the crack tip mechanisms play the dominant role. These approaches involve the use of different variables and diagrams, but also reflect different philosophies. In order to provide a common frame it is useful to analyse the general mechanical scheme in Fig. 1. For a generical fracture propagation experiment, the external load can be represented by a given force F , displacement X or traction velocity V applied to a loading point. In the most general case, the test sample can be subdivided into a series of regions that progressively transfer the energy to the crack tip, such as the body, the process zone (one or a series of shells depending on the number of potential dissipative mechanisms), a local near-tip elastic enclave, and the region inside the crack cavity. The mechanical role of each of these regions is schematically represented in the block diagram in Fig 2, where the nature of each block can change between different materials, each one possibly being elastic, viscoelastic, viscoplastic, etc (the symbols used in the graph are just evocative!). In order for K to be definable and the LEFM to apply, the body block should be purely elastic and the process zone size should be small with respect to the sample and fracture length sizes. According to the theory for brittle materials (Lawn 1983), it is possible to define a small enclave zone near the crack tip that behaves in an essentially elastic way and that allows the definition of the local values of G^* and K^* that are relevant for describing crack tip processes.

In the first approach (mainly formalised by Maugis (1985) to describe fracture in polymers and peeling of adhesives) fracture propagation in a given material is generally characterised by $G(v)$ curves, representing the strain energy release rate as a function of the crack velocity (Fig. 3). This makes it particularly easy to consider the energy balance of fracture propagation in relation to the time scales of deformation solicited by different crack propagation velocities. In this formalism, the low velocity limit can be identified with the 'equilibrium' surface energy $G_0 = 2\gamma_0$. Then the fracture energy increases with velocity due to enhanced activation of concomitant irreversible dissipative processes, which determine a stationary propagation curve in the form $G(v)$. For the case of viscoelastic materials, the slow fracture region is generally in the form of a power law

‡ The present review is limited to mode I tensile fracture for simplicity, the variable K will stand for K_I

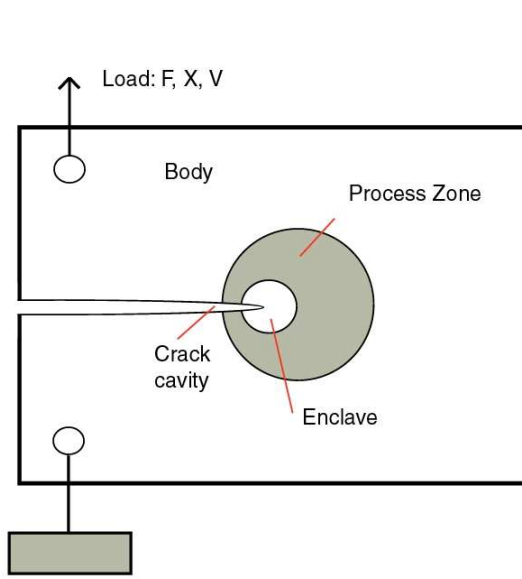


Figure 1. Graphic representation of the mechanical elements for fracture mechanics.

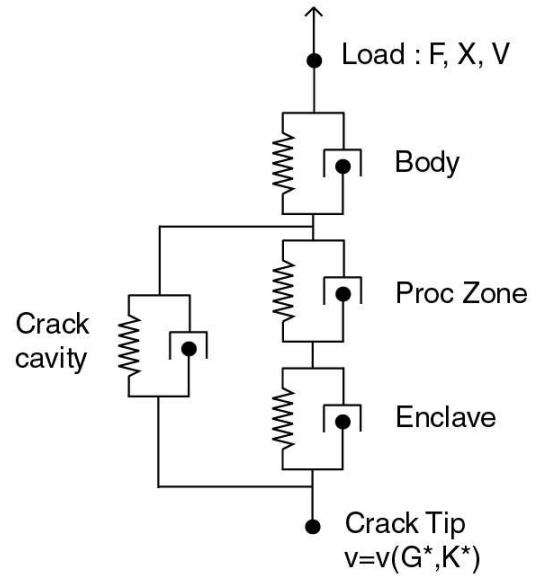


Figure 2. Symbolic block representation of the different mechanical elements.

of the kind $G(v) = G_0(1 + A_T v^n)$, where A_T includes the temperature dependence. The increasing portion of the $G(v)$ curve eventually ends at some critical velocity v_c , where the dissipative process starts to be less and less effective, since the kinetic scale becomes faster than the viscoelastic relaxation. For higher velocity the fracture energy increases again due to the manifestation of dynamic effects (Freund 1990) eventually leading to a divergence when the crack velocity approaches the sound propagation velocity[§]. The presence of a maximum in the $G(v)$ curve leads to an intrinsic mechanical instability in the fracture propagation dynamics for a critical value G_c that should not be confused with the threshold surface energy $G_0 = 2\gamma_0$, although it is generally proportional to it. The range of velocities corresponding to a negative slope in the $G(v)$ curve is not allowed for stationary crack propagation and generally leads to stick-slip dynamics (c.f. Ciccotti *et al* 2004). The instability at G_c , i.e. the jump from slow to rapid fracture for a constant applied force, is of particular interest since it is marked by a sharp reduction of the amount of energy dissipated by fracture propagation, letting all the excess furnished energy be converted to kinetic energy with the typical emission of acoustic bursts (Barquins and Ciccotti 1997).

In the second approach (mainly developed by the works of Wiederhorn on glass and formalised by Lawn (1993) for brittle materials) the accent is focused on the kinetics of a crack tip debonding process as a function of the applied stresses. The fracture propagation curves are generally represented by $v(K)$ curves, where the crack propagation velocity is considered as a variable dependent on the stress intensity factor

[§] The observed limit propagation velocity is generally only a fraction of the sound velocity due to the occurrence of other kinds of dynamical instabilities (c.f. the review of Fineberg and Marder 1999).

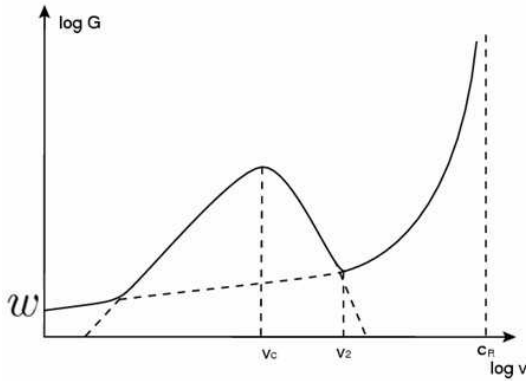


Figure 3. Typical $G(v)$ diagram for crack propagation in polymers and adhesives ($w = G_0$).

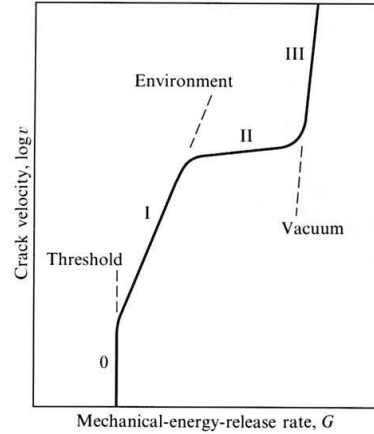


Figure 4. Typical $v(K)$ or $v(G)$ diagram for subcritical crack propagation in glass.

(Fig. 4). The global energy balance is somehow in a subsidiary position, and the fracture kinetics is determined by the rate of thermal activation of a generic discrete bond breaking reaction (Thomson *et al* 1971) whose activation energy is reduced by the application of stresses, leading to an Arrhenius like exponential equation $v = v_0 \exp[-(\Delta E_a - bK)/k_B T]$, that may also be expressed in terms of G (c.f. section 3.1). In this interpretation, the critical value K_c for the transition to dynamic propagation should correspond to the end of the lattice trapped regime, while the equilibrium surface energy $2\gamma_0$ should correspond to an eventual propagation threshold (c.f. section 3.4). However, this basic modelling can only be argued for fracture in vacuum (or for a single debonding mechanism), since at ambient condition the slow crack propagation in glass is complicated by the chemical reactions. We should however retain that the position of the critical value K_c is rather related to the discreteness and heterogeneity of the material than to a surface energy, since it represents the moment where the energy barriers for individual break bonding tend to zero. In materials which are heterogeneous on a large scale, this approach can be reposed based on a larger basic grain size (Broberg 2003).

The two approaches can be interestingly combined in brittle materials presenting a non negligible process zone, yet allowing for the definition of a small near-tip elastic enclave. For doing that we should first assume that the local values of G^* and K^* in the enclave are effective in ruling the crack tip propagation kinetics according to a relation $v(K^*)$ (Lawn 1983). In the absence of forces inside the crack cavity, the energy dissipated in the process zone can be evaluated by the difference $G - G^*$ (by applying the J integral formalism of Rice 1968) and will cause both G^* and K^* to be smaller than their macroscopic counterpart G and K . The effect of energy dissipation will thus translate into a shielding (or local relaxation) of the crack tip stresses. The presence of generalised force into a limited portion of the near-tip crack cavity will also act as a shielding factor at the crack tip, and it may involve or not energy dissipation depending on the nature of the interaction.

When describing the macroscopic fracture properties of a material, it is the relation of the external variables G, K which is studied as a function of v . Even if assuming a uniquely defined kinetic law $v(G^*, K^*)$, these local variables remain hidden, and the presence of a process zone will cause the non-unicity of the macroscopic fracture laws $v(G, K)$. This induces a time- or crack-length dependent behaviour (R-curve) that may lead into controversial interpretation (Lawn 1993). These kinds of modelling will be shown later to be particularly effective in rationalising the propagation threshold behaviour.

As a concluding remark to this section, it is generally useful to identify the different space and time scales of each symbolic block (c.f. Fig. 2) in order to estimate if the different dissipation mechanisms will have time to activate and how they will influence the energetic balance or the fracture propagation laws. Several spatial scales are present in the problem, such as the sample lateral dimensions and thickness, the loading displacement, the crack length, the basic grain size of the material (molecular rings for glass), the size of the process zone (or of each shell of a multiple process zone), the enclave size, the length of the one or several cohesive zones in the crack cavity. Typical time scales are given by the loading or displacement rate, the crack velocity, the stimulation time of each equivalent block and its characteristic relaxation time, the rate of thermal activation of different mechanisms, the rate of transport of different relevant chemical species in the bulk or in the crack cavity. We will try to keep these space and times scales in mind while proceeding in the description of the crack propagation kinetics in glasses and especially when trying to get a deeper insight on the stress-corrosion mechanisms.

3. Crack propagation kinetics

A huge amount of possible oxide glasses may be created by melting together variable amounts of oxides, within specific compositional ranges that are strongly influenced by the quench speed (c.f. Zarzycki 1991). The details of the chemical reactions and the competition between different propagation mechanisms will be altered, but many typical features of crack propagation remain substantially similar. The most influent difference is between glasses essentially made by network former oxides (SiO_2 , GeO_2 , B_2O_3 , P_2O_5 , etc.) and glasses containing significant amounts of modifier oxides (Na_2O , K_2O , CaO , etc.). For that reason in the following the silica glass will mainly be described as representative of the first class and a typical soda-lime glass will be used as paradigm to represent the second class of glasses.

The subcritical fracture propagation properties of glasses are generally studied using samples that allow for a mostly stable slow propagation of a single fracture such as the Double Torsion (DT, Evans 1972), the Dual Cantilever Beam (DCB, Srawley and Gross 1967) or the Double Cleavage Drilled Compression (DCDC, Janssen 1974). The measurement of the crack propagation velocity as a function of the applied stress intensity factor generally presents three (or four) characteristics regions like in Fig. 4.

3.1. Zone I: stress-corrosion regime

In zone I, corresponding to the stress-corrosion regime, the crack propagation velocity is a strongly increasing function of the stress intensity factor K , it has an almost linear dependence on humidity in moist air (Fig. 5) and it increases with temperature (Fig. 6). All these dependencies can generally be fitted by the Wiederhorn (1967) equation:

$$v^I = v_0 \exp(\alpha K) = A \left(\frac{p_{H_2O}}{p_0} \right)^m \exp \left(-\frac{\Delta E_a - bK}{RT} \right) \quad (1)$$

where p_{H_2O} is the partial pressure of the vapour phase in the atmosphere, p_0 is the total atmospheric pressure, and R the gas constant; A , m , ΔE_a and b are four adjustable parameters that take into account the dependence on the glass composition.

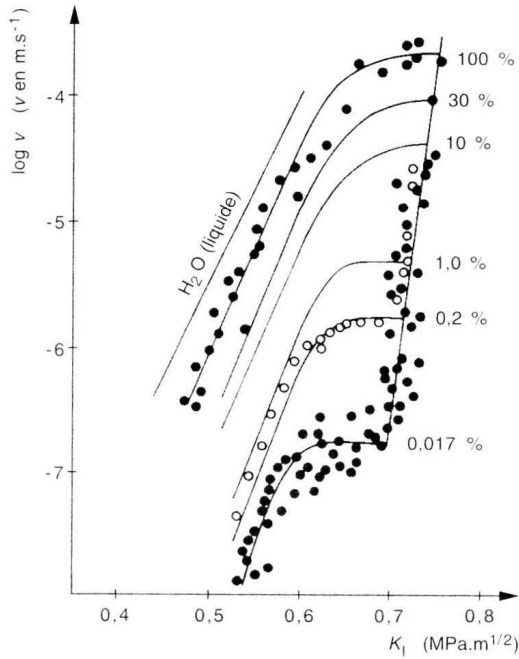


Figure 5. Effect of humidity on the crack propagation in soda-lime glass (from Wiederhorn 1967).

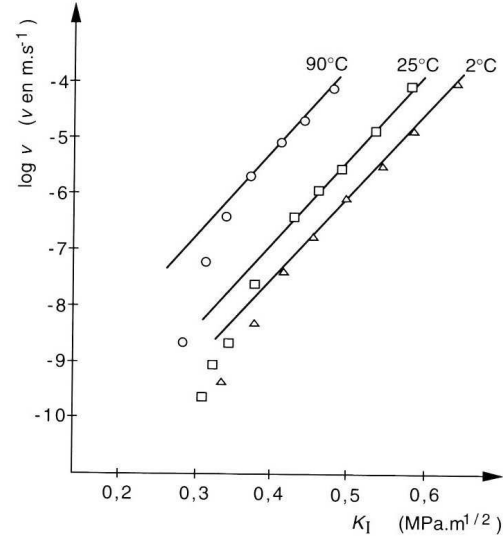


Figure 6. Effect of temperature on the crack propagation in soda-lime glass (from Wiederhorn and Bolz 1970).

However, due to the extremely elevated dependence of velocity on the stress intensity factor K and to the limited range of variation of K , the data in zone I may also be fitted by power a law expression like in the Maugis (1985) approach:

$$v^I = v_0 (K/K_0)^n \quad (2)$$

the exponent n being generally between 12 and 50 for silicate glasses (Gy 2003). This form is by the way particularly useful (and indeed used) for developing simple analytical predictions of the time of life in static and dynamic fatigue tests (Varner 2006). The difficulty in determining the most adequate relation results in a strong uncertainty in the predictions over very long periods.

For the same reasons, the zone I data can also be fitted by a different exponential equation proposed by Pollet and Burns (1977) and applied to glasses by Lawn (1993):

$$v^I = v_0 \exp(\alpha G) = A \exp\left(-\frac{\Delta E_a}{k_B T}\right) \exp\left(-\frac{\alpha(G - G_0)}{k_B T}\right) \quad (3)$$

where the energetic balance has a more central role, as it will be discussed later concerning the threshold at G_0 .

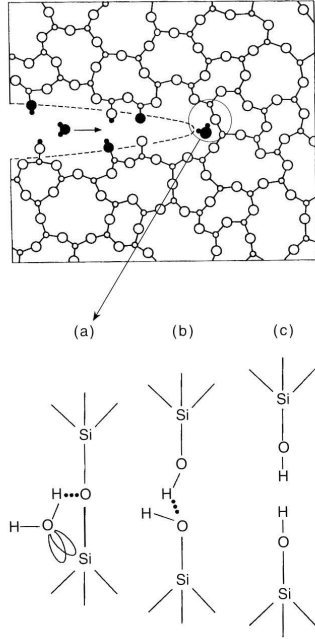


Figure 7. Basic mechanism of the stress-corrosion reaction (from Michalske and Bunker 1984).

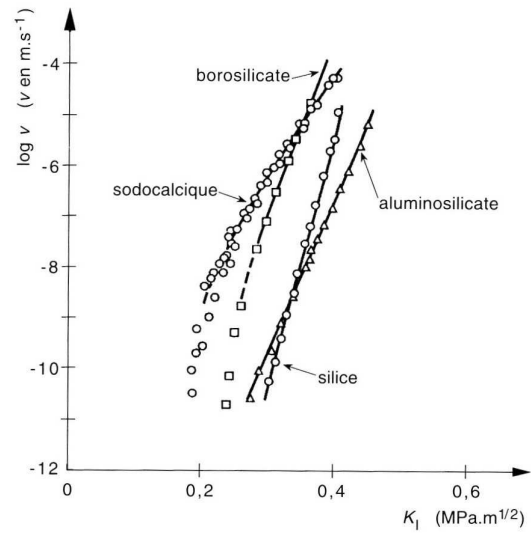


Figure 8. Effect of glass composition on the crack propagation in soda-lime glass (from Wiederhorn and Bolz 1970).

The Wiederhorn equation (1) has been the most used in the description of zone I in glasses since it provides a more direct interpretation of the chemical reactions between a glass of a given composition and the environment at the crack tip. In this framework, the basic mechanism of the stress-corrosion reaction was associated to the stress-enhanced thermal activation of a dissociative hydrolysis reaction represented in Fig. 7 for the case of silica glass. Michalske and Bunker (1984) supported the positive effect of stress on the reaction rate by a molecular-orbital simulation of the reaction on distorted siloxane bonds. They later provided experimental support to their theory by measuring the rate of hydrolysis of a series of strained silicate ring structures (Michalske and Bunker 1993). For other glass compositions (Fig. 8), several other reactions are possible, but they share the similar feature of being stress-enhanced and thermally activated, thus explaining the exponential (Arrhenius like) term in equation (1), where ΔE_a can be interpreted as an activation enthalpy in the absence of stress and b can be expressed in

terms of an activation volume (of molecular dimensions) by relating the stress intensity factor to the crack tip stress (Wiederhorn and Bolz 1970). According to the chemical reaction rate theory (Glasstone *et al* 1941), the preexponential term represents the activity of the reactants in the moist atmosphere and the exponent m (generally close to 1) is related to the nearly first order of the stress-corrosion reaction (Wiederhorn *et al* 1974).

For propagation in liquid environment, the term p/p_0 is substituted by the activity of water molecules which is strongly dependent on the composition of the liquid environment. Notably, it is strongly affected by the pH and ionic concentration of some species related to the glass composition (Wiederhorn and Johnson 1973). Apart from water, other molecules that are effective for stress-corrosion such as ammonia, hydrazine and formamide have in common (a) the capability of donating both a proton and an electron at the two ends of the molecule and (b) a molecular diameter inferior to 0.5 nm (Michalske and Bunker 1987). The first property is necessary to present a concerted reaction of adsorption and scission of the siloxane bridges of the glass network (Fig. 7, bottom). The small diameter is necessary for the reactive molecules to be able to reach the strained bonds at the crack tip without steric problems. The effect of other non reactive liquids is mainly that of reducing the effective concentration of water to traces and thus of substantially suppressing the stress-corrosion propagation (Freiman 1975) in a similar way to the propagation in dry nitrogen or in vacuum.

3.2. Zone II: transport limited propagation

In zone II the crack propagation velocity is substantially independent on the stress intensity factor (Fig. 5), since the reaction rate is limited by the transport kinetics of reactive molecules towards the crack tip. The plateau value for propagation in moist air is increased when increasing humidity in qualitative accord with the proposed equation (Wiederhorn 1967):

$$v^{II} = v_0 p_{H_2O} D_{H_2O} \quad (4)$$

where D_{H_2O} is the diffusion coefficient of water molecules in air. However, a finer analysis reveals that several mechanisms can act in limiting the transport of the reactive molecules as a function of the environment (total pressure, humidity, temperature, liquid or vapour form of the water molecules) and of the progressive confinement experienced when approaching the crack tip (Lawn 1993). The diffusion of water molecules in a vapour or solute will be first reduced by the decrease of the average free path, and then possibly by the activated adsorption on the crack walls when the confinement becomes of the same order as the molecular size. While the first mechanism is mostly acknowledged for glasses (Michalske and Bunker 1987), the second one is likely to be determinant in the cleavage of mica under humidity (Wan, Aimard *et al* 1990).

Zone II is very limited in liquid water, and the extension of the zone II in glass was shown to be reduced at elevated humidity (Wan, Lathabai *et al* 1990) suggesting the

presence of capillary condensation in the crack cavity. In liquid solutions, the position of zone II depends on the water concentration, and a zone II plateau remains generally visible in a very low velocity region for inert liquids or gases due to trace amounts of water as discussed above (Freiman 1975). Water molecules may also penetrate the strained glass network in a molecular form (Deremus 2002) and react with the network in a more internal location near the crack tip (Marsh 1964b; Tomozawa 1996). In this case the bulk diffusion rate could also act as a limiting factor in zone II. However, most of these phenomena are expected to depend in a similar manner from temperature and stress (c.f. section 4.1), making their distinction difficult by only measuring $v(K)$ curves.

3.3. Zone III: inert propagation and failure

When reaching zone III, the crack propagation velocity starts increasing again with K (Fig. 5). The dependence is so steep that the measurements require special techniques, such as the modulation of the fracture surface generated by sound waves (Gehrke *et al* 1991). The position of the zone III is substantially independent on the local environment, in agreement with the expected suppression of the stress-corrosion reactions. The propagation in vacuum or in inert liquids or gases allows to extend the zone III domain down to very low velocities (Wiederhorn *et al* 1974). These delicate measurements showed that the $v(K)$ curves are still temperature dependent and that they can be fitted with an Arrhenius relation with a more elevated activation volume.

Although the velocity is rapidly climbing to large values, the propagation is still of a subcritical type, i.e. the time scale for crack propagation is still determined by the time required from thermal fluctuations to overcome the weaker and weaker energy barriers. According to lattice trapping models (Thomson *et al* 1971), the critical stress intensity factor K_c represents the end of the region III, i.e. the moment where no more energy barriers exist and the mechanical energy is converted into kinetic energy in an unstable manner, the time scale for propagation being now determined by dynamic equations. However, due to the elevated slope of region III in glasses and to the elevated values of the crack velocity, it is hardly possible to establish experimentally the end point of region III and the value of K_c is generally identified with the position of region III itself. On a practical point of view, when loading a sample in tension, the sample will generally fail abruptly when approaching K_c , and the measured value is called the fracture toughness. On the other hand, in stable fracture configurations ($dK/dc < 0$) such as the DCDC specimen, and in the absence of stress-corrosion (for example in vacuum or in nitrogen) the crack will simply arrest for $K = K_c$ and further propagate only upon increase of the load.

The toughness of silicate glasses is generally around $0.8 \text{ MPam}^{1/2}$, and it can range in a $\pm 20\%$ interval between most typical glass compositions (Vernaz 1978)||. The

|| We should remark that the corresponding fracture energy of glass in inert atmosphere is of the order of $G_c = 2\gamma_f = K_c^2/E' \simeq 8 \text{ J/m}^2$, which is ten fold higher than the typical values of the surface tension of glasses $\gamma_0 \simeq 0.5 \text{ J/m}^2$ (c.f. sect. 4.3).

relation between K_c and glass composition is quite complex since the glass network structure is strongly affected by the percent amount of each oxide (Vernaz 1978). Since the toughness is generally related to the Young modulus, according to the estimation $K_c = \sqrt{\gamma E}$, the compositions with higher young modulus are generally tougher. Another apparently consistent correlation appears between the decrease of toughness and the number of non-bridging oxygen atoms, that is determined by the amount of modifier oxides (Rizkalla *et al* 1992). Moreover, the toughness tends to increase when decreasing the size of the alkali ion in ternary glasses (Gehrke *et al* 1991), suggesting the importance of ion migration even in the rapid fracture (c.f. section 4.5). However, a clear comprehension is still lacking, and several research efforts are still being done to establish more clear correlations. The major reason for this delay is that the measurements of K_c are quite delicate and that they are generally obtained with very different techniques, the overall scattering being comparable with the observed effects.

3.4. Zone 0: threshold behaviour, healing and aging

In some glasses, such as alkali rich glasses, a threshold behaviour occurs (Fig. 9), i.e. fracture velocity rapidly falls to undetectably low values when K decreases toward a threshold value K_s (Gehrke *et al* 1991). This property is of extreme importance in the life duration of engineering glass products, yet its origin is very subtle and has long been subject of debate.

According to Griffith theory, a threshold for propagation should exist at $G = G_0$ where $G_0 = 2\gamma_0$ represents the thermodynamic surface energy which is necessary to create the new surfaces through the cohesive bond breaking. In the framework of the rate reaction theory (Glasstone *et al* 1941) this equilibrium condition corresponds to the equality of the rates of the two opposite reactions of breaking and recombination. The crack propagation velocity in proximity of such equilibrium threshold can thus be approximated by including in Eq. (3) a term for the rate of recombination:

$$v = v_0 \exp \left(-\frac{\Delta E_a - \alpha(G - G_0)}{k_B T} \right) + v_0 \exp \left(-\frac{\Delta E_a + \alpha(G - G_0)}{k_B T} \right) \quad (5)$$

$$= v_0 \exp \left(-\frac{\Delta E_a}{k_B T} \right) \sinh \left(\frac{\alpha(G - G_0)}{k_B T} \right)$$

Equation (5), besides presenting a threshold for propagation at $G = G_0$, also implies the backward propagation or healing of the crack for $G < G_0$, in agreement with the thermodynamical considerations of Rice (1978)¶.

However, this scenario is not exactly what is happening with glass. For soda-lime glass, although the crack propagation stops at a threshold $G_s \simeq 0.4 \text{ J/m}^2$, no healing is observed down to a lower value $G_c \simeq 0.15 \text{ J/m}^2$ (c.f. Fig. 10), suggesting that the

¶ We should remark that we can only talk about reversible crack propagation for $G \approx G_0$, i.e. for vanishing propagation velocity, while both forward and backward propagation with finite velocity imply a rate of energy dissipation $(G - G_0)v \geq 0$.

closure happens due to a different mechanism than the opening, such as the hydrogen bond interaction between hydrolysed crack surfaces (Stavrinidis and Holloway 1988). For silica glass, although no propagation threshold G_s is observed down to $v = 10^{-13}$ m/s (Muraoka and Abé 1996), crack closure also happens for a value of G_c similar to that of soda-lime glass. Moreover, the repropagation kinetics is quite different in the two kinds of glasses. While repropagation of the healed crack in silica happens as soon as $G \geq G_c$, the repropagation threshold G'_s in soda-lime progressively increases between G_c and G_s as function of the time spent in the closed configuration (Stavrinidis and Holloway 1988), suggesting partial reformation of the siloxane bridges (Michalske and Fuller 1985).

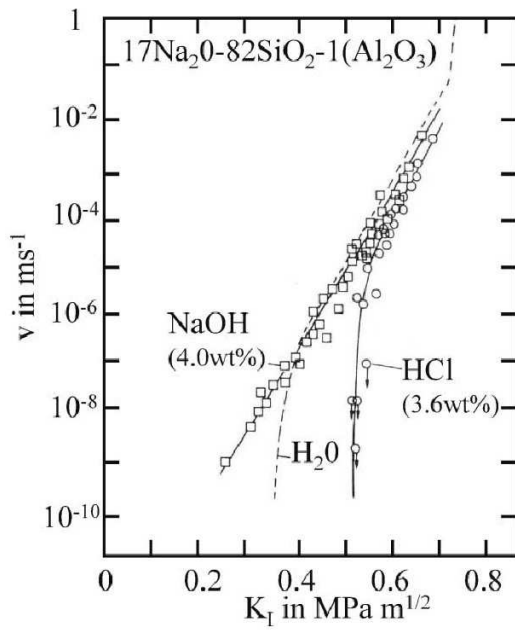


Figure 9. Threshold behaviour in a sodium-alumono-silicate glass in water and in solutions with different pH (from Gehrke *et al* 1991).

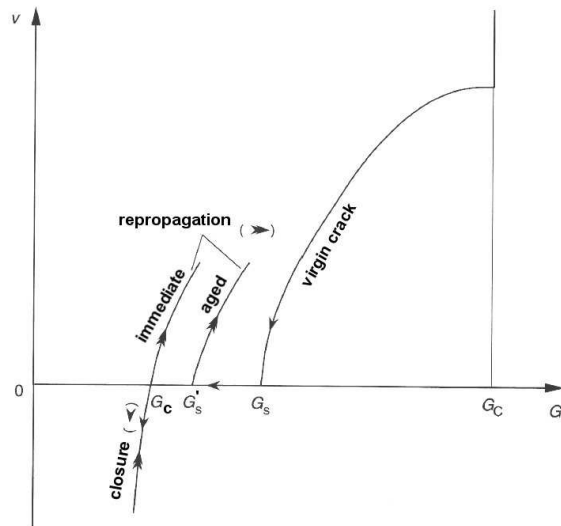


Figure 10. Sketch of the hysteretic healing and repropagation behaviour in soda-lime glass.

This phenomenon should not be confused with another kind of aging that can be observed in soda-lime glass. When the crack is arrested and held for a given time at a value G_h in the interval $G_c < G_h < G_s$ (NB: without healing), the repropagation will not start again at G_s , but it will either need the application of a higher value of G , or to wait for a delay time which is maximum when $G_h \simeq G_s$ (Michalske 1977, Gehrke *et al* 1991).

The threshold behaviour and the delayed fracture after crack arrest in alkali containing glasses were shown to be deeply related, and can be interpreted as a consequence of the ion exchange phenomenon (Gehrke *et al* 1991; Fett *et al* 2005a). Ion exchange at the crack tip and at crack surfaces can have several effects: (a) the

build up of compressive stresses at the crack tip, shielding the external stresses, (b) a change of the surface energy and/or a dissipation of energy that can alter the energetic balance, (c) a change of the local glass composition leading to an increase of the fracture resistance. This interpretation was supported by the strong dependence of the threshold and arrest time for soda-lime in liquids on the pH of the solution and glass composition in a series of binary and ternary glasses (Fig. 9). An acidic solution (*HCl*) enhances the ion exchange and causes the threshold to shift to upper values of G_s , while a basic solution (*NaOH*) can make the threshold reduce below the detection limit. A specific exception is observed in glasses with high alkali content, where the corrosion behaviour is so rapid that fracture propagates spontaneously presenting a horizontal plateau on the $G(v)$ curve for a low limit velocity around 10^{-7} m/s, especially in presence of an acidic solution (Gehrke *et al* 1991).

The phenomenon of ion exchange will be discussed more deeply in sections 4.1 and 4.5 since the effect of local stresses plays an important role, and the discussion of the difference of behaviour between the propagation in water and in moist atmosphere requires a more detailed analysis of the chemical processes in confined liquid films. However, some considerations are opportune here. The hysteretic behaviour of the crack closure and repropagation in soda-lime glass, as well as the non observation of any threshold in silica, cast strong doubts on the applicability of the Griffith scenario for reversible healing in glasses. The hydrolysis reaction of the siloxane bonds is essentially irreversible at ambient temperature, and the crack closure at G_c rather involves the adhesion of the hydrated crack surfaces (the latter being rather reversible for silica). For alkaline glasses, the modifications of the crack surfaces are even more drastic due to the irreversible production of ion exchange layers. The position of the threshold G_s is thus not easily associable with a glass surface energy in the Griffith sense, but it is rather the effect of the competition between the kinetics of the formation of the ion exchange layer and the crack propagation kinetics. It is however difficult to disregard the similarity between the typical values of $G_s \sim 0.8$ J/m² and the estimates of the glass surface tension, both being about one tenth of the fracture energy in inert environment. This seems to suggest that the complex interaction of glass with water during slow fracture helps the glass surface to relax from the elevated non equilibrium energies towards its equilibrated condition.

4. A deeper insight in the stress-corrosion and damage mechanisms

4.1. Competition between dissolution, corrosion and leaching

In order to understand more deeply the different components of the chemical contribution of water molecules to the corrosion and damage of glass, the three main categories of reactions that can occur between glass and an aqueous solution should be reexamined (c.f. Bunker 1994 for a more detailed review): (1) hydration consists of the penetration of molecular water into the glass network as an intact solvent; (2)

hydrolysis and condensation are the two opposite chemical reactions which break or reform the $Si - O - Si$ (or equivalent) network bonds by exchange with a couple of hydroxyl groups according to the scheme:



(3) ion-exchange reactions consist of the replacement of a modifier cation (such as sodium) by a hydrogen or hydronium ion:



Silicate glasses are essentially soluble in water (Iler 1979), yet the dissolution reaction is so slow at ambient condition that glasses are considered as exceptionally inert materials, and generally need tens of years exposure to moisture before showing significant surface alteration. However, when increasing temperature or stress these reactions can be significantly accelerated, especially under extremely acid or basic environmental conditions. Moreover, if the three reactions occur at the same time, each reaction will influence the kinetics and mechanisms of the other reactions (Bunker 1994).

In pure silica glass only the first two reactions are possible and they cooperate in the water diffusion kinetics. According to the reactive diffusion model developed by Doremus (well reported in his book of 2002), water mainly diffuses in molecular form with a well defined thermally enhanced diffusion coefficient, but it continuously reacts with the glass network being thus temporarily immobilised in the $SiOH$ form. As a result, an effective water diffusion coefficient can be defined that also depends on concentration. At elevated temperature, the water content converges to the equilibrium solubility (mainly dependent on the free volume in glass network) and the hydrolysis reaction is equilibrated (mainly towards the dissociated state). However, at lower temperatures close to ambient condition, the reactions are not equilibrated and both hydroxyl and molecular water are present in the glass with a very complex speciation, which is often subject of debate (Stuke *et al* 2006; Doremus 2002).

In alkali containing glasses such as soda-lime, water diffusion is greatly complicated by the combination with the ion exchange reactions (Doremus 1975). Since alkali ions partly fill the network voids, ion exchange can be the limiting factor for water diffusion, but hydrolysis is also necessary to open the pathways in the glass network (Bunker 1994). Lanford *et al* (1979) have shown that alteration layers are formed on glass surfaces in liquid water by selective leaching of alkali ions. The layer width is initially proportional to the square root of time (diffusion controlled process) and eventually reaches a stationary value due to the equilibration with the slow etching of the glass surface. The hydrated layers that are formed on soda-lime glass were shown to be depleted of sodium in a proportion that suggests the substitution of sodium ions with the hydronium ions H_3O^+ (rather than the hydrogen ion). This exchange is responsible of the development of a stressed surface layer depending on the relative volume difference

of the exchanged ions. In the case of soda-lime glass the developed stress is compressive, in agreement with the hypothesis of a sodium/hydronium exchange, the volume of hydronium and hydrogen being respectively larger and smaller than that of sodium. In an analog manner the exchange of sodium with the larger potassium ions is induced in the chemical tempering treatments to enhance the strength of glass products (see Gy 2008 for an extensive review). The composition and structure of the leached layer are thus heavily altered and are more similar to a hydrated silica glass than to the initial glass. Moreover, under extensive leaching, the recondensation reactions can also become important actors of a more profound restructuration of the glass network leading to the formation of a more compact glass phase, similar to anhydrous silica glass, pervaded by a more permeable porous network, often called a gel layer (Bunker 1994).

While the behaviour and thermodynamics of these corrosion processes have been extensively studied as a function of temperature, pH and composition of the liquid in contact with the glass surface (c.f. the review of Conradt 2008), the behaviour under moist atmosphere is often more subtle (Bunker 1994) due to the formation of thin nanometric water films on glass surfaces whose detailed chemistry escapes present state thermodynamics and often entails the formation of complex patterns (Watanabe *et al* 1994). Moreover, although these reactions are known to be strongly influenced by the local stress state, the accurate study of their behaviour at elevated tensile stresses is still lacking and is subject of great debates. The next sections will try and make more clear the present knowledge about the consequences of these behaviours in the damage processes near the crack tips, where the extremely elevated stress gradients affect smaller and smaller zones, thus making the space and time scales of the different mechanism be deeply variable and interdependent.

4.2. Crack tip blunting

If we go back to the sharp-crack atomic-bonding paradigm, this really means that at room temperature the rate of hydrolysis of individual crack-tip bonds, which are singularly enhanced by the elevated crack tip stress, is the only relevant process for determining the crack tip propagation laws (c.f. Fig. 7). Or at least that this remains the case once we have identified the stress intensity factor K^* in the local enclave, thus admitting the possibility that the other processes and reactions be effective in a surrounding process zone (Fig. 1). This hypothesis constitutes a singular (degenerate) state of the original Charles and Hilligs (1962) theory, in which the stress-enhanced corrosion rate cannot act any more in sharpening the crack tip since its curvature radius has reached its inferior limit, estimated to 0.5 nm and corresponding to the radius of the basic siloxane rings of the glass network.

This conditions of propagation at constant tip radius is the ground base for the interpretation of the Wiederhorn equation (1) in terms of the LEFM theory and for the uniqueness of the $v(K^*)$ curve (Lawn, 1983). However, this can not apply to the description of the initial growth of blunt flaws to become sharp cracks, and we can

wonder if this would be the only possible destiny for the progressively sharpening cracks in all conditions. Can the final crack tip radius of curvature be a function of K at least for some glass and/or environment composition? Can the competition between the rate of the different processes and the crack tip velocity make the crack tip so blunt (or 'effectively' blunt due to material damage) that it may stop under an apparently elevated value of K (i.e. larger than what expected by the glass surface energy)? The debate on this subject has been especially active concerning the origin of the propagation threshold and of the crack closure/aging/repropagation behaviour (plasticity issues will be discussed in section 4.3).

Since the solubility of glass surfaces is also dependent on the local radius of curvature (Iler 1979), when the external stresses are very low the crack walls should be corroded more rapidly than the tip, leading to a progressive tip blunting effect (Ito and Tomozawa 1982). Moreover, the presence of a gradient of solubility in a very confined environment can lead to a concomitant phenomenon of dissolution from the lateral walls and reprecipitation at the crack tip, which would even enhance the extent of the tip blunting (c.f. Fig. 11), as observed in a controversial TEM study of the crack tip in silica (Bando *et al* 1984). If such blunting happens in an almost static condition, then the fracture should be substantially reinitiated after reloading, leading to an effect of temporary increase of the glass strength, which was proposed as an alternative explanation to the occurrence of a time delay before repropagation of aged fractures (Han and Tomozawa 1989).

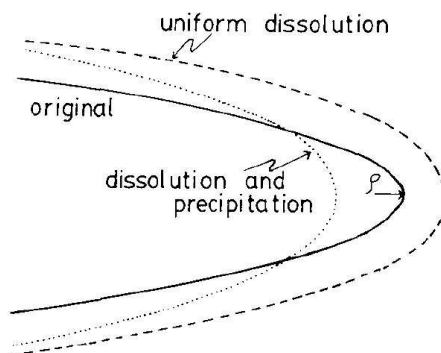


Figure 11. Schematic representation of the blunting mechanisms (from Ito and Tomozawa 1982).

The difficulty in this debate originates from different causes. On one hand, since all these reactions are influenced by stress, temperature and pH, the extent and rapidity of occurrence of these phenomena is strongly dependent on the specific condition and on both the glass and environment composition, making the comparison of different experiments more subtle, especially if we take into consideration the difference between the behaviour in water and in moist atmosphere. On the other hand, several conclusions were based on the indirect effect of these phenomena on the measurements of strength of glass samples subjected to different kinds of treatments (Han and Tomozawa 1989).

A condition which has often been shown to lead to several superposed effects on the flaw distribution and nature in the glass, but also on the local state of the residual stresses which deeply affect this kind of measurements. For example, in the case of the aging of indentation flaws, the experiments of Lawn *et al* (1985) suggest that the strength increase during aging is caused by the relaxation of the indentation residual strains (also produced to a variable extent when finishing the glass surface) by subcritical crack propagation of the flaws.

Fett *et al* (2005b) have recently modelled quantitatively the strength increase of an uncharged soda-lime glass plate after inducing a surface compression layer by ion exchange in water at 90 °C and obtained good agreement with experimental measurements. They also made an analog model for the effects of the formation of an ion exchange layer in the internal crack walls and tip neighbourhood of both static and propagating cracks in a soda-lime glass in water (Fett *et al* 2005a). This model supports the interpretation of the threshold behaviour by the effect of the compressive stresses induced in the ion exchanged layer. They finally compared (by AFM *post-mortem* recombination) the mismatch in the morphology of the crack surfaces obtained after inducing the partial corrosion of the crack walls of an arrested crack in soda-lime glass (Guin and Wiederhorn 2005) and letting the crack repropagate to failure. The comparison reveals a homogeneous corrosion of the two faces and is argued as an evidence of the sharp nature of the crack tip at the propagation threshold.

Although these measurements are quite convincing for the case of the specific soda-lime glass, the applicability to all conditions requires more systematic works of this kind. It is generally accepted that after extreme corrosive attack (such as after HF etching) the cracks are very likely to be blunted as proposed by Proctor (1962). However, several intermediate conditions may exist where the elevated susceptibility of some kinds of glass to dissolution induces an anomalous propagation behaviour as in the high alkali binary glasses studied by Gehrke *et al* 1991 or in some alumino-phosphate glasses (Etter *et al* 2008).

4.3. Crack tip plasticity

Another major objection to the sharp-crack atomic-bonding paradigm comes from the hypothesis of a significant contribution of plastic deformation at the crack tip in the slow crack propagation mechanisms. Since the early works of Dugdale (1960) on metals, and the observations of plastic behaviour of glass under compression in indentation and scratch marks (Taylor 1949), several investigations have been carried out to track the evidence of plastic behaviour in the strong tensile stress field at crack tips in glasses. In particular, Marsh (1964a; 1964b and refs there in) edited a series of papers developing a complete theory of elasto-plastic fracture propagation theory for glass, which was proposed as an alternative to the Griffith explanation for brittle glass strength and to the Charles-Hilligs interpretation of static fatigue as the effect of stress-corrosion.

The theory closely follows the formalism developed by Dugdale for metals, defining

as a suitable fracture criterion the formation of a plastic zone of critical dimensions $R \simeq 6$ nm for typical glasses having a yield stress of about 10 GPa. The occurrence of static fatigue is explained as a contribution of the stress-enhanced water diffusion into the glass to a local reduction of the glass viscosity and thus of the resistance to plastic flow (Marsh 1964b). The time scale for fracture propagation is thus attributed to the transport of water in bulk glass and to the consequent viscous flow, although the kinetics is not explicitly developed.

Wiederhorn (1969) performed accurate measurements of the fracture energy for six glasses in inert environment and showed that once the stress-corrosion is suppressed, the fracture energies $\gamma_f = G_c/2$ range between 3.5 and 5.3 J/m², a figure which is ten fold higher than the typical values of the surface tension of glasses $\gamma_0 \simeq 0.5$ J/m² estimated by Griffith (1921) and which suggests a major contribution of irreversible processes in crack propagation. By analysing the implications of the plastic model proposed by Marsh (1964b), Wiederhorn estimated a plastic work of 4.5 J/m², and he observed that although it is in rough agreement with the measured fracture energies it is very small compared to that obtained in metals of 10⁴ J/m². Moreover, since all the estimated space scales for the local deformations are close to the dimensions of the molecular scale (the average size of glass network rings is of the order of 0.5 nm), he questioned the opportunity of applying the concept of 'plasticity' to the nanoscale.

On the other hand, the sharp-crack atomic-bonding paradigm that was advocated by Lawn (1983) as the foundation of the brittle fracture theory, considers that load be borne in a completely elastic way at the molecular level. According to this hypothesis only the molecules at the direct end of the molecularly sharp crack tip are broken sequentially under the elevated load. Lawn *et al* (1980) conducted an extensive evaluation of this possibility by comparing the nature of the atomic bonds and structure between glasses and other brittle or ductile materials. They supported their conclusion on the absence of plastic behaviour in glasses demonstrating by TEM observations the absence of dislocations in crystalline oxides with same composition (as opposed to more ductile crystals).

However, the hypothesis of Marsh (1964b) went well beyond the discussion of fracture in inert atmosphere and vacuum conditions. Marsh was well aware that water is the oxide which has the highest effect in lowering the viscosity of a glass melt (c.f. Del Gaudio *et al* 2007) and his explanation of the effect of humidity on the slow crack propagation (as an effect of reduced glass viscosity by stress-enhanced diffusion of water into the glass) was intended as a completely alternative mechanisms of stress-corrosion. By looking at this interpretation with more modern eyes, the basic mechanism remains indeed similar, since the reduction of glass viscosity is likely to be caused by a stress-enhanced hydrolysis of the network siloxane bridges, substituted with more mobile *SiOH* terminations. However, this hydrolysis would not be limited to the crack tip rings, but rather involve a larger process zone, likely of the order of a few tens of nanometers, corresponding to a region with an effective yield stress of 1 GPa. The model is also quite different in that the time scale is not simply governed by the rate of

reaction at the tip, but also by the rate of stress-enhanced diffusion of water into the glass and the time scale of structural relaxation which is accelerated by both stress and the reduced viscosity due to hydration. This would lead to a process zone size that is a decreasing function of the crack velocity and thus of K .

The development and experimental investigation of a similar scenario was progressively carried on by Tomozawa and collaborators in the eighties using IR and Raman spectroscopies to detect water diffusion profiles in silica glass and the consequent changes in the glass structure, identified by changes of the so called 'fictive temperature'⁺. A good review of this work can be found in Tomozawa (1996). However, some relevant points will be recalled here. Ito and Tomozawa (1981) initially observed an increase in the dissolution rate of silica glass under hydrostatic pressure at 285°C, and argued that the opposite should happen in tension, in contrast to the stress-corrosion hypothesis of Charles and Hilligs (1962). On the other hand, Nogami and Tomozawa (1984) showed that the water diffusion into glass was exponentially enhanced on the tensile side of a bent plate of silica glass under saturated moist atmosphere at 192 °C (the opposite occurring on the compressive side), the hydrated layer reaching a thickness of several microns after 300 h. These two combined observations led Tomozawa to suggest that glass structural relaxation caused by stress-induced water penetration at the crack tip could be an alternative mechanisms for slow crack propagation in glass. However, most measurements were done at high temperature and the extrapolation to ambient condition is generally difficult due to non equilibrated reactive diffusion and to difficulties in estimating the solubility, especially due to reported trend inversions at different temperatures. A major advancement was provided by Tomozawa *et al* (1991) who measured by resonant nuclear reaction analysis the enhanced water entry into silica glass fracture surfaces during slow crack growth at ambient temperature. The thickness of the hydrated layer at ambient condition was estimated to about 10 nm which is of the order of the experimental resolution, but the increase in the amount of water is significant when compared to crack propagation in inert environment. The support for the overall model has progressively advanced through several complementary observations, which are necessary to separate and test the effect of the water content, the fictive temperature and the applied stress. Peng *et al* (1997) have documented the effect of stress and water content in accelerating the surface structural relaxation in silica fibers. Li *et al* (1995) have shown that silicate glasses with higher fictive temperature present both greater

⁺ Glass being an out of equilibrium material, its structure and properties are not uniquely determined by the thermodynamical variables, but also depend on the past thermal history. According to the hypothesis of Tool (1946), the thermal history may be represented by the knowledge of a unique additional variable named the fictive temperature T_f . This variable represents the temperature of the supercooled equilibrated glass melt which has the same structure as the present glass. For the same composition, a higher fictive temperature corresponds in general to a lower density and index of refraction. When a glass is aged at a temperature $T' < T_f$, its structure undergoes a slow evolution toward the equilibrated state, the relaxation time being inversely proportional to the glass viscosity. During this relaxation the fictive temperature decreases towards the value of T' . However, in practice it is quite difficult to equilibrate glasses to a fictive temperature less than 900 °C.

fatigue resistance and inert strength. Koike and Tomozawa (2006) showed that the fictive temperature also affects differently the subcritical crack growth rate of silicate glasses and soda-lime glasses.

The bibliography on this subject is very rich and can not be reviewed in detail here. Several observation and especially some interpretations have been longly debated and are still disregarded by the 'sharp-tip' community, since once again they are based on many indirect observations and extrapolations from different temperatures and other conditions. Moreover, the thermal treatments to change the fictive temperature are not without effects on the flow distributions and the effects on strength should be taken with great care. However, this mechanisms remain largely plausible and would need a major synthetic effort to prove its real effectiveness for crack propagation in silica (and especially in other glasses) at ambient condition. Such modelling should end in the writing of kinetic equations that may fit the experimental data as well as the Wiederhorn equation (1) and that provide a physical interpretation for the model coefficients which be related to measurable quantities.

A different series of investigations were made possible by the application AFM techniques in glass science in the '90s. In 1996 Guilloteau *et al* made first *in-situ* AFM measurements of the external glass surface during crack propagation in borosilicate glass. They observed the presence of a surface depression ahead of the crack tip, and they estimated the presence of a process zone of 50 nm size (corresponding to a yield stress of 1 GPa) by identifying the deviation of the vertical displacement profiles from the power law predictions of linear elasticity. Similar results were obtained by Célarié *et al* (2003) on lithium aluminosilicate glasses and by Prades *et al* (2005) on silica glass, by *in-situ* AFM observation of slow fracture propagation in DCDC samples under pure mode I. The process zone size was observed to grow in size from 20 to 100 nm when the propagation velocity diminished from 10^{-10} to 10^{-12} m/s due to a decrease of K . Moreover, these AFM measurements suggested that the crack propagation in the process zone proceeds by the nucleation, growth and coalescence of nanometric cavities, in a sort of similar way to what happens in the ductile fracture of metals at the micrometer scale.

These observations reopened the debate on crack tip plasticity, which is presently very active due to several contradicting evidences. Lopez-Cèpero *et al* (2007) have observed that the *post-mortem* recombination of the AFM measurements of the morphology of opposite crack surfaces in silica and soda-lime showed no evidence for the expected traces of the nanocavities in the bulk of the specimen. Moreover, Fett *et al* (2008) showed the inadequacy of the 2D plane-stress solution of Maugis (1992) used by Guilloteau *et al* (1996) and then by Célarié *et al* (2003) to represent the elastic vertical surface displacement near the crack tip with a $r^{-1/2}$ dependence. When using the correct r^λ dependence (with $\lambda \simeq 1/2$), which was derived by Bazant and Essentoro (1979) to describe the corner singularity of a 3D surface striking crack (c.f. Dimitrov *et al* 2006), the deviation of the displacement profiles measured by AFM from the elastic solution is much less evident (Fett *et al* 2008). The quality of the fit on the vertical

topography profiles is deeply affected by the presence of the surface roughness even if this is indeed very low due to excellent polishing. Moreover, the combination of the roughness and the crack tip surface deformation could origin features very similar to the cavities observed by Célarié *et al* 2003 as shown by numerical simulation (Fett *et al* 2008).

However, all these measurements are very close to the instrumental limits of the AFM topographical images which are made with AFM tips of an average radius of 10 nm. Better insights could be obtained by succeeding in the difficult task of separating the vertical surface displacement from the surface roughness by using digital image correlation techniques (Hild and Roux 2006). Moreover, a signature of the occurrence of inelastic processes during crack propagation can be searched in the statistical correlation functions of the crack surface morphology (c.f. section 4.6).

The recent development of complementary techniques to measure the crack tip stress fields with nanometric resolution are also very promising for determining the effective scale of a damage process zone. We can cite the SEM cathodo-luminescence measurements (Zhu *et al* 2007; Pezzotti *et al* 2008) and the promising measurements by nanoRaman and EBSD techniques (Cook 2008).

4.4. Local crack tip environment

Since the kinetic propagation in the stress-corrosion regime is strongly affected by the environment in the crack tip cavity, and since this is a highly confined region with a typical crack opening ranging from 0.5 nm at the tip to a few nanometers a distance of 1 μm , it is questionable that the local crack tip environment can be treated as equivalent to the outer environment, be it liquid or gaseous, and also that the macroscopic description of the thermodynamic state of the environment at a nanometric confined crack tip be relevant.

The zone II behaviour is a first sign of inhomogeneous crack tip environment. Since water is being used by the crack tip for propagation, the local concentration (in gaz or solute) at the crack tip is considered to decrease when the crack tip velocity is comparable with the transport rate of water in the cavity. The near tip concentration in zone II was modelled to fall near zero (Wiederhorn 1967), and the concentration gradient established in the crack cavity would be the motor for water diffusion to the crack tip, it's rate becoming the controlling factor for crack propagation (c.f. section 3.2). On the other hand, when the whole sample is sunk in water, a more subtle issue is given by the viscous transport of liquid water toward the tip. This transport is indeed very effective since the zone I only starts changing its slope when near to zone III. However, at elevated velocity, a pressure drop at the tip may be caused by the increasing viscous drag, leading eventually to a negative pressure in the crack tip region. A very interesting investigation by Michalske and Frechette (1980) has suggested that a strongly negative pressure can be sustained at the crack tip without cavitation due to the elevated confinement, leading to the observation of a supercritical crack propagation

at limited velocity, that can be interpreted according to the shielding effect (reduction of K^*) caused by the internal forces in the crack cavity (c.f. Fig. 1). A further increase of K eventually leads to cavitation in water when the negative pressure extends to a less confined region of the crack cavity, followed by an instantaneous order of magnitude rise in the crack velocity due to the sudden depletion of the crack tip environment and to the release of the internal forces. A similar cavitation-induced dynamical instability was observed by Maugis (1985) in brittle polymers.

In alkali containing glasses in water, the enhanced leaching at the crack tip may cause a local change of the liquid composition at the crack tip. This was suggested to be the cause of an observed transition in the slope of the zone I in soda-lime glass (Wiederhorn and Johnson 1973). At low crack velocity the crack tip environment would be equilibrated to the external liquid composition, while becoming more related to the crack tip reactions at higher velocity. The same kind of effect can be supposed for other type of corrosion products, such as silicic acid, but still has to be quantified.

Recent AFM *in-situ* observations have shown that nanometer scale capillary condensation occurs at crack tips in silica glass in moist air for crack velocities between 10^{-12} and 10^{-9} m/s (Wondraczek *et al* 2006; Ciccotti *et al* 2008). This liquid phase is made stable by the short range interaction with the glass surfaces under elevated confinement and constitutes a major alteration of the local environmental condition at the crack tip with respect to the gaseous hypothesis (Wiederhorn 1967). In this condition, not only the water is readily available at the crack tip, but the local pressure becomes strongly negative due to the Laplace pressure, thus exerting a strong attractive force between the crack lips and altering the equilibrium of the stress-corrosion reactions. Since the crack-tip reaction rate is expected to depend on the chemical activity of water, and the condensate was shown to be in equilibrium with the humid atmosphere (Grimaldi *et al* 2008), we can expect that the humidity dependence of the crack velocity remains similar to what expected in gaseous environment, yet the situation should change when transport phenomena become relevant or when the equilibrium is questioned. For example, the liquid condensate can be an explanation of the reduction of the transport limited zone II region observed at elevated humidity (Wan, Aimard *et al* 1990). The end of the condensate being in a less confined region than the crack tip, the limiting factor for the diffusion of water in the gas phase should be progressively inhibited.

The liquid condensation was also observed on alkali containing glasses (Célarié *et al* 2007) and should in this case have a much larger effect since the local compositional changes, due to the crack tip enhanced leaching, can not be diluted in a bulk liquid. Preliminary results show that the extent of the condensation in soda-lime glass is significantly enhanced by the alterations due to the local leaching (c.f. section 4.5). The relevance of capillary condensation in the propagation kinetics of phosphate glasses, which are less resistant against dissolution, can be seen in the anomalous temperature behaviour observed in the $v(K)$ relations measured by Crichton *et al* (1999) and similarly by Etter *et al* (2007) at ambient temperature. The anomaly is suppressed at higher

temperature where the condensation can not form.

4.5. Alkali ion migration under stress gradient

In section 4.1 we have seen that chemically driven sodium ion migration can happen spontaneously at soda-lime glass surfaces thus inducing a local state of compression in a surface hydrated layer. Gorsky (1935) first showed that the opposite can also be true, i.e. that a strong stress gradient can induce sodium migration towards the tensile direction of the gradient. While the spontaneous slow flow is generally balanced by interchange with other positive ions (such as the hydronium ion) in order to preserve charge neutrality (Doremus 1975; Lanford *et al* 1979), the behaviour under a strong stress gradient is less evident. Weber and Goldstein (1964) measured a transient electric current between the tension and compression sides of a bent soda-lime slide, indicating that the non-balanced flow can be settled up before being counteracted by the build up of an opposite electric potential difference. Moreover, Langford *et al* (1991) have revealed intense sodium emission after rapidly fracturing soda-lime glass in vacuum. The delay in the emission was of the order of a few tens of milliseconds, indicating that sodium migration can be very fast in the presence of strong stress gradients and can thus also affect region III water-free fast crack propagation. Several observations were made concerning an excess sodium concentration in the outermost surface layer of fracture surfaces in soda-lime, followed by a sodium depleted region of larger thickness of hundreds of nanometers (Pantano, 1985). This phenomenon looks similar to the chemically driven migration, however its space and time scales are quite different and more investigation is needed about the interaction of this phenomenon with the external environment during and after the fracture process.

Watanabe *et al* (1994) made an interesting AFM investigation of the time evolution of the fracture surfaces of a soda-lime glass broken in low vacuum at a velocity of 10^{-3} m/s (zone III) and then aged in ambient moist atmosphere. The excess concentration of sodium on the fracture surfaces is the cause of an unusually rapid corrosive action on these surfaces, observable by the appearance of protuberances and swellings interpreted as the recondensation of corrosion products in the form of a weak sodo-silicate gel material. The evolution of such swellings under common atmosphere finally evolves to the formation of carbonatic crystallites due to the interactions with CO_2 dissolved in the sodium rich wet layers.

A similar kind of alteration has been observed by imaging external surfaces in the neighbourhood of a crack tip produced by indentation on a soda-lime slide (Nghiem 1998). More recently, Célarié *et al* (2007) have conducted a systematic *in situ* AFM study of the kinetics of the growth and evolution of the protuberances during crack propagation in soda-lime under controlled atmosphere of nitrogen and variable humidity levels. The absence of CO_2 have allowed focussing on the space and time scales of the sodium exchange mechanisms and of the surface corrosion process. The region affected by the surface swellings is shown to have a parabolic shape which is modelled

according to the competition between the spreading of the surface reaction and the crack propagation velocity (Fig. 12). The parabolic shapes for different crack velocities at 45% RH are consistent with a diffusive process with an effective diffusion coefficient of the order of $1 \text{ nm}^2/\text{s}$, which is an increasing function of the relative humidity. The application of phase imaging techniques has also allowed to identify the thickening of the sodium enriched liquid layer (predicted by Watanabe *et al* 1994) prior to the manifestation of the swellings.

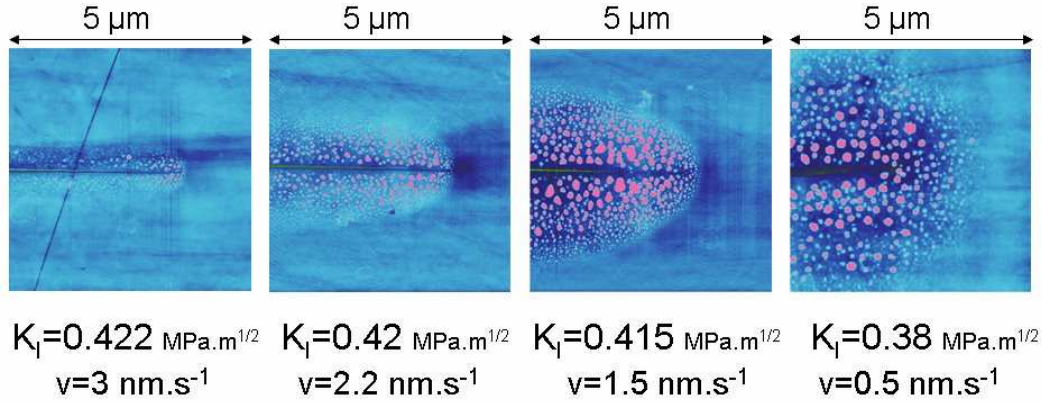


Figure 12. AFM topographical images of a propagating crack in soda-lime glass at different crack velocities for RH=45%.

When fracture velocity slows down below 10^{-9} m/s the ion exchange front can spread ahead of the crack tip and thus start relaxing the tensional stresses in the crack tip region, which in turn will cause the progressive arrest of the crack propagation. This suggests the extension to the propagation in moist atmosphere of the interpretation of the threshold behaviour proposed by Michalske and Bunker (1985). The enhanced liquid condensation stimulated by the sodium enrichment at the fracture surfaces and in the parabolic front plays the role of the bulk liquid reservoir, but its elevated degree of confinement let it act very differently, like in the observations of Watanabe *et al* (1994). The space and time scales for the spreading of the ion exchange can be quite different.

Fett *et al* (2005a) modelled the mechanical effect caused by the chemical induced ion exchange layer forming on the crack surfaces and at the crack tip of arrested and propagating cracks in soda-lime glass. This modelling is based on the ion exchange kinetics proposed by Lanford *et al* 1979 for an etched soda-lime surface in water at pH7. The lateral extension of the parabolic front predicted by this model would be about 1000 smaller than the one observed in Fig. 12. The extremely different scales can be attributed on one side to the discussed difference of the propagation in moist air (and the consequent change in the composition of the condensed liquid layers), and on the other side to the influence of the strong stress gradient at the crack tip, which is not accounted in the model of Fett *et al* (2005a).

4.6. Fracture surfaces

As we have seen throughout this review, *post-mortem* study of the fracture surfaces is an excellent complementary tool to understand the physics and chemistry of the mechanisms of crack propagation. On one side, the morphology of the fracture surface can contain relevant information on the dynamics of crack propagation and on the traces of inelastic processes and of the corrosion of the crack surfaces. On the other side, modern high resolution chemical probes can provide invaluable insights on the understanding of the nature of these high energy surfaces and thus of the mechanisms that originated them (Pantano 1985).

The fracture surface morphology has long been used to draw informations about the origin and propagation of the cracks that led a glass specimen to failure. An optical inspection allows distinguishing the three typical zones of increasing roughness called 'mirror', 'mist' and 'hackle' and which correspond to progressive crack acceleration from subcritical to dynamic propagation (Johnson and Holloway 1966). The spread of AFM investigations in the '90s has shown that surface roughness in the 'mirror' zone is of the order of a fraction of nm (RMS) when measured on micrometer size images and that it is almost comparable with the roughness of melt surfaces and with the best levels of surface finishing by polish treatments (c.f. Rädlein and Frischat 1997; Arribart and Abriou 2000).

The dependence of the RMS roughness of fracture surfaces in the mirror region on the glass nature was extensively studied to understand the relation between the heterogeneities in the glass composition and the crack path through the glass (Gupta *et al* 2000; Wiederhorn *et al* 2007). Other investigators have explored the scaling properties of the fracture surfaces (Bouchaud 1997) and investigated the dependence of the self-affine exponents and the characteristic cutoff length from the velocity of crack propagation (Bonamy *et al* 2006).

The extensive development of dynamical models for the dynamics of the crack front line in a heterogeneous material (c.f. Ramanathan *et al* 1997), have made the investigation of the scaling behaviour of glass fracture surfaces a mostly interesting tool for probing the physics of crack propagation. A particularly interesting aspect is the suggested correlation between the position of some cutoffs length in the scaling properties with the size of the process zone as observed in several different materials (Bonamy *et al* 2006), which support the idea that a generalised process zone behaviour can affect scales of the order of a few tens of nanometers during slow crack propagation in silica, the size of the process zone being an increasing function of the decreasing crack propagation velocity.

A complementary useful tool to study the extent of the damage mechanisms induced by crack propagation is the study of the mismatches in the recombination of the two opposite fracture surfaces. Guin *et al* 2004 showed that it is possible to match down to nanometer scale opposite fracture faces of a soda-lime glass broken in water. The fine comparison on a few sections normal to the crack surface showed no evidence

of 10 nm sized damage cavities in the bulk of the glass sample (c.f. also Fett *et al* 2008). However, the determination of the remnants of damage processes on *post-mortem* (unstressed) fracture surfaces requires extreme care since the relevant information is at the nanometer scale and the metrologic capacities of AFM images are generally affected by several delicate problems such as drifts, feedback effects, noise and tip shape artifacts (Flemming *et al* 2005). The accurate treatment of these kinds of problems will benefit of the present development of digital image correlation techniques (Hild and Roux 2006) and requires the application of advanced statistical estimation tools.

As discussed in section 3.4, *post-mortem* AFM investigations and recombination techniques have also led to important insights in the nature of the threshold of propagation and of the mechanisms of crack arrest and aging. For example, Guin *et al* 2005 could measure with this technique the extent of the dissolution of the crack surfaces when a crack in soda-lime glass is loaded near the propagation threshold into a basic solution. The work of Watanabe *et al* 1994 on the evolution of the fracture surfaces of a soda-lime glass after fracture in vacuum has provided a great insight in the time scales of the corrosion mechanisms caused by the subsequent interaction with the moist atmosphere.

The UHV AFM investigations of the fracture surfaces of different kinds of glasses with molecular resolution (Frischat *et al* 2004) have provided an intimate view of the complex nanostructures in multi-component glasses and their role in the slow crack propagation processes. These kinds of measurements are very promising for relating the fine structural measurements in bulk glasses (Wright 2008) with the molecular simulations of the peculiar structure of the glass fracture surfaces (Du and Cormack 2005; Roder *et al* 2001).

Many techniques for the high resolution characterisation of the structural and chemical properties of glass surfaces are being developed, which are out of the scope of the present review. I will just cite here some relevant investigation of the hydroxylation behaviour of fracture surfaces (Souza and Pantano 2002) since the study of the water adsorption sites and of the mechanisms and time scales of hydroxylation are of particular interest in the understanding of the high energy nature of the glass fracture surfaces (Leed and Pantano 2003) and in the modelling of the wetting properties of fracture surfaces, which were shown to have a paramount role in the corrosion mechanisms in moist environment (c.f. section 4.5).

5. Perspectives

After almost one hundred years from the initial insights on the nature of the brittle crack propagation in glasses we finally feel the flavour of a turning point in the comprehension of the basic mechanisms of slow crack propagation in glasses. The kernel of the difficulty turned to be the fact that there are many actors playing in the opera, most of them acting at the nanoscale and in a deeply interrelated manner. The amorphous nature of glass has deprived the scientists of most of their typical modelling and characterisation tools,

and the exceptional degree of homogeneity of glass relegated all the relevant phenomena to the nanoscale, where the chemical nature of surfaces becomes mostly relevant and the elevated degree of confinement makes even the traditional thermodynamics fail. Even the disordered structure of both the glass network and the reactive molecules (such as water) tend to turn to ordered at the nanoscale, a fascinating order that is often peculiar to each of the many glass compositions.

The turning point comes from the progressive adequation to the nanoscale of both the investigation tools, the simulation techniques and the increasing comprehension of the physics of the nanoworld. Different kinds of local scanning probes have allowed the visualisation of the space and time scales of the physico-chemical mechanisms during crack propagation or in the subsequent evolution of the crack surfaces. Several structural and compositional analysis are also increasing their resolution and reducing the severity of their condition of use. The most promising developments concern the progressive development of setups combining different complementary probes capable of tracking different phenomena on a single test (such as AFM+microRaman techniques). At the same time, the gap between simulation and experience is being drastically reduced. On one side, both molecular dynamics and first principle simulations are permitting to explore increasing volumes of matter and for increasing time durations (which remain however the limiting point). On the other side several experiments in UHV conditions are exploring physical conditions that approaches to what is really simulated (by exploring for example the interaction of few water molecules with glass fracture surfaces).

On another standing point, the separation between the crack tip and process zone phenomena and the behaviour of a glass sample as a more complex structure have been well captured by adequate mechanical modelling and expert researchers are now aware of the issues related to the management of residual stresses, of surface finishing, of the relevance of surface corrosion and leaching and of the importance of the surface conditioning treatments on the modification of the surface flaws and flaw nucleation sites.

A major observation through this review stands in the deep difference between the crack propagation and surface corrosion processes in liquid solutions and the occurrence of the same phenomena under moist atmosphere. While the first case corresponds to an overall controlled environment (at least for slow crack propagation), in the second case the local environment at the crack tip and at the glass fracture and external surfaces is determined by a very confined condensation layer which can significantly evolve in time. CO_2 in the atmosphere was also shown to be a major actor in the evolution of the different chemical reactions. It is thus of fundamental importance to dispose of an elevated degree of control of the atmosphere during the investigations, and to make separate studies of these phenomena under pure mixtures of nitrogen and humidity.

This review is not exhaustive, but hopefully sufficient analysis should have been provided in order to promote a deep reflection on the relevance of the different actors. This reflection should step by identifying the space and time scales of action of the

different physical and chemical processes in the close neighbourhood of the crack tip and of the crack surfaces as a function of the different glass compositions and controlled environments. This should always be complemented by the estimation of the separate energetic contribution of the single mechanisms. A special attention should be paid to the complete characterisation of the glass samples used, including their detailed composition, structural and mechanical properties and the definition of the thermal history as well as the details of the surface finishing techniques. The reproducibility of the results in different laboratories will be key point of a real understanding.

We should not forget that understanding the nature of the crack propagation mechanisms will help in solving just a part of the problem of glass strength. This should be combined with a comprehension of the flaw nucleation mechanisms starting from different kinds of defects in glass and with the development of techniques making glass objects more tolerant to the presence of such flaws. Strong efforts in these sense are being invested by both the academic and industrial communities in order to make glass a promising material for advanced applications in the XXI century.

Acknowledgments

This work was motivated by the reflections on the animation of the Technical Committee TC09 on Glass Nanomechanics in the International Commission on Glass and by the organization of a workshop financed by the EFONGA project that will take place in 2009 in Montpellier. The research activity was financed by the ANR project CORCOSIL (BLAN07-3_196000). I thank all the TC09 and TC19 members for nice discussions as well as the colleagues of the Glass group in Montpellier and the partners of our ANR project in CEA-Saclay and Université Lyon I. A special thanks to M. George for critical reading of the manuscript and to C. Marlière and F. Célarié for initially developing the Nanomechanics activity in Montpellier.

References

- Arribart H and Abriou D 2000 *Ceramics-Silikáty* **44** 121–8
- Bando Y, Ito S and Tomozawa M 1984 *J. Am. Ceram. Soc* **67** C36–7
- Barenblatt G I 1962 in *Advances in Applied Mechanics* vol 7 (New York: Academic Press) pp 55–129
- Barquins M and Ciccotti M 1997 *Int. J. Adhes. Adhes.* **17** 65–8
- Bazant Z P and Estenssoro L F 1979 *Int. J. Solids Struct.* **15** 405–26
- Bouchaud E 1997 *J. Phys.: Condens. Matter* **9** 4319–44
- Bonamy D, Ponson L, Prades S, Bouchaud E and Guillot C 2006 *Phys. Rev. Lett.* **97** 135504
- Broberg K B 2003 *Strength, Fracture and Complexity* **1** 31–8
- Bunker B C 1994 *J. Non-Cryst. Solids* **179** 300–8
- Célarié F, Ciccotti M and Marlière C 2007 *J. Non-Cryst. Solids* **353** 51–68
- Célarié F, Prades S, Bonamy D, Ferrero L, Bouchaud E, Guillot C and Marlière C 2003 *Phys. Rev. Lett.* **90** 075504
- Charles R J and Hillig W B 1962 in *Symp. on Mechanical Strength of Glass and Ways of Improving It* Florence, Italy, September 25–29, 1961 (Charleroi, Belgium: Union Scientifique Continentale du Verre) pp 511–27

- Ciccotti M, George M, Ranieri V, Wondraczek L and Marlière C 2008 *J. Non-Cryst. Solids* **354** 564–8
- Ciccotti M, Giorgini B, Vallet D and Barquins M 2004 *Int. J. Adhes. Adhes.* **24** 143–51
- Conradt R 2008 *J. Am. Ceram. Soc.* **91** 728–35
- Cook R F 2008 Private communication
- Crichton S N, Tomozawa M, Hayden J S, Suratwala T I, Campbell J H 1999 *J. Am. Ceram. Soc.* **82** 3097–104
- Del Gaudio P, Behrens H and Deubener J 2007 *J. Non-Cryst. Solids* **353** 223–36
- Dimitrov A, Buchholz F G and Schnack E 2006 *Comp. Model. Eng. Sci.* **12** 1–25
- Doremus R H 1975 *J. Non-Cryst. Solids* **19** 137–44
- Doremus R H 2002 *Diffusion of Reactive Molecules in Solids and Melts* (New York: John Wiley & Sons)
- Du J and Cormack A N 2005 *J. Am. Ceram. Soc.* **88** 2532–39
- Dugdale D S 1960 *J. Mech. Phys. Solids* **8** 100–4
- Etter S, Despetis F and Etienne P 2008 *J. Non-Cryst. Solids* **354** 580–6
- Evans A G 1972 *J. Mater. Sci.* **7** 1137–46
- Fett T, Guin J P and Wiederhorn S M 2005a *Eng. Fract. Mech.* **72** 2774–91
- Fett T, Guin J P and Wiederhorn S M 2005b *Fatigue Fract. Eng. Mater. Struct.* **28** 507–14
- Fett T, Rizzi G, Creek D, Wagner S, Guin J P, López-Cepero J M, and Wiederhorn S M 2008 *Phys. Rev. B* **77** 174110
- Fineberg J and Marder M 1999 *Phys. Rep.* **313** 1–108
- Flemming M, Roder K and Duparré A 2005 *Proc. SPIE* **5965** 59650A:1–10
- Freiman S W 1975 *J. Am. Ceram. Soc.* **58** 339–41
- Freund L B 1990 *Dynamic Fracture Mechanics* (Cambridge: Cambridge University Press)
- Frischat G H, Poggemann J F and Heide G 2004 *J. Non-Cryst. Solids* **345** 197–202
- Gehrke E, Ullner C and Mahnert M 1991 *J. Mater. Sci.* **26** 5445–55
- Glasstone S, Laidler K J and Eyring H 1941 *The Theory of Rate Processes* (New York: McGraw-Hill)
- Gorsky W S 1935 *Phys. Zeit. Sowjet.* **8** 457–71
- Griffith A A 1921 *Phil. Trans. Roy. Soc. London* **A221** 163–198
- Grimaldi A, George M, Pallares G, Marlière C and Ciccotti M 2008 *Phys. Rev. Lett.* **100** 165505
- Guilloteau E, Charrue H and Creuzet F 1996 *Europhys. Lett.* **34** 549–53
- Guin J P and Wiederhorn S M 2004 *Phys. Rev. Lett.* **92** 215502
- Guin J P and Wiederhorn S M 2005 *J. Am. Ceram. Soc.* **88** 652–59
- Gupta P K, Inniss D, Kurkjian C R and Zhong Q 2000 *J. Non-Cryst. Solids* **262** 200–6
- Gy R 2003 *J. Non-Cryst. Solids* **316** 1–11
- Gy R 2008 *Mater. Sci. Eng. B* **149** 159–65
- Han W T and Tomozawa M 1989 *J. Am. Ceram. Soc.* **72** 1837–43
- Hild F and Roux S 2006 *Strain* **42** 69–80
- Iler R K 1979 *The Chemistry of Silica* (New York: John Wiley and Sons)
- Irwin G R 1960 in *Mechanical and Metallurgical Behavior of Sheet Material* (Proc. 7th Sagamore Ordnance Materials Research Conf., Syracuse) (Arlington, Virginia: ASTIA) pp IV.63–71
- Irwin G R and Washington D C 1957 *J. Appl. Mech.* **54** 361–4
- Ito S and Tomozawa M 1982 *J. Am. Ceram. Soc.* **65** 368–71
- Janssen C 1974 in *Proc. 10th Int. Cong. on Glass (Kyoto)* (Tokyo, Japan: Ceramic Society of Japan) pp 10.23–10.30
- Johnson J W and Holloway D G 1966 *Phil. Mag.* **14** 731–43
- Koike A and Tomozawa M 2006 *J. Non-Cryst. Solids* **352** 5522–30
- Lanford W A, Davis K, Lamarche P, Laursen T, Groleau R, Doremus R H 1979 *J. Non-Cryst. Sol.* **33** 24966
- Langford S C, Jensen L C, Dickinson J T and Pederson L R 1991 *J. Mat. Res.* **6** 1358–68
- Lawn B R 1983 *J. Am. Ceram. Soc.* **66** 83–91
- Lawn B R 1993 *Fracture of Brittle Solids* 2nd ed (Cambridge: Cambridge University Press)

- Lawn B R, Hockey B J and Wiederhorn S M 1980 *J. Mat. Sci.* **15** 1207–23
- Lawn B R, Jakus K and Gonzales A C 1985 *J. Am. Ceram. Soc.* **68** 25–34
- Leed E A and Pantano C G 2003 *J. Non-Cryst. Solids* **325** 48–60
- Li H, Agarwal A and Tomozawa M 1995 *J. Am. Ceram. Soc.* **78** 1393–6
- López-Cepero J M, Wiederhorn S M, Fett T and Guin J P 2007 *Int. J. Mat. Res.* **98** 1170–6
- Marsh D M 1964a *Proc. R. Soc. London Ser. A* **279** 420–74
- Marsh D M 1964b *Proc. R. Soc. London Ser. A* **282** 33–43
- Maugis D 1985 *J. Mater. Sci.* **20** 3041–73
- Maugis D 1992 *Eng. Fract. Mech.* **43** 217–55
- Michalske T A 1977 in *Fracture Mechanics of Ceramics* vol 5 ed R C Bradt, A G Evans *et al* (New York: Plenum Press) pp 277–89
- Michalske T A and Bunker B C 1984 *J. Appl. Phys* **56** 2686–93
- Michalske T A and Bunker B C 1987 *J. Am. Ceram. Soc.* **70** 780–4
- Michalske T A and Bunker B C 1993 *J. Am. Ceram. Soc.* **76** 2613–8
- Michalske T A and Frechette V D 1980 *J. Am. Ceram. Soc.* **63** 603–9
- Michalske T A and Fuller E R 1985 *J. Am. Ceram. Soc.* **68** 586–90
- Muraoka M and Abé H 1996 *J. Am. Ceram. Soc.* **79** 51–7
- Nghiem B 1998 PhD Thesis. Université Paris-VI, France
- Nogami M and Tomozawa M 1984 *J. Am. Ceram. Soc.* **67** 151–4
- Orowan E 1955 *Weld. J. Res. Suppl.* **34** S157–160
- Pantano C G 1985 in *Strength of Inorganic Glass (Nato Conference Series VI)* ed C R Kurkjian (New York: Plenum Press) pp 37–66
- Peng Y L, Tomozawa M and Blanchet T A 1997 *J. Non-Cryst. Solids* **222** 376–82
- Pezzotti G, Leto A and Porporati AA 2008 *J. Ceram. Soc. Japan* **116** 869–74
- Pollet J C and Burns S J 1977 *Int. J. Fract.* **13** 775–86
- Prades S, Bonamy D, Dalmas D, Bouchaud E, Guillot C 2005 *Int. J. Solids Struct.* **42** 637–45
- Proctor R 1962 *Phys. Chem. Glasses* **3** 7–27
- Rädlein E and Frischat G H 1997 *J. Non-Cryst. Solids* **222** 69–82
- Ramanathan S, Ertas D and Fisher D S 1997 *Phys. Rev. Lett.* **79** 873–6
- Rice J R 1968 *J. Appl. Mech.* **35** 379–86
- Rice J R 1978 *J. Mech. Phys. Solids* **26** 61–78
- Rizkalla A S, Jones D W and Sutow E J 1992 *Br. Ceram. Trans. J.* **91** 12–15
- Roder A, Kob W and Binder K 2001 *J. Chem. Phys.* **114** 7602–14
- Souza A S and Pantano C G 2002 *J. Am. Ceram. Soc.* **85** 1499–504
- Srawley J E and Gross B 1967 *Mater. Res. Std.* **7** 155–62
- Stavrinidis B and Holloway D G 1983 *Phys. Chem. Glasses* **24** 19–25
- Stuke A, Behrens H, Schmidt B C and Dupré R 2006 *Chem. Geol.* **229** 64–77
- Taylor E W 1949 *Nature* **163** 323–3
- Thomson R, Hsieh C and Rana V 1971 *J. Appl. Phys.* **42** 3154–60
- Tool A Q 1946 *J. Am. Ceram. Soc.* **29** 240–53
- Tomozawa M 1996 *Annu. Rev. Mater. Sci.* **26** 43–74
- Tomozawa M, Han W T and Lanford W A 1991 *J. Am. Ceram. Soc.* **74** 2573–6
- Varner J 2006 *Strength and fracture mechanics of glass in: ICG Advanced Course 2006: Strength of Glass, Basic and Test Procedures* (Offenbach, Germany: Verlag DGG) pp 23–37
- Vernaz E 1978 PhD thesis, Université Montpellier 2, France
- Wan K T, Aimard N, Lathabai S, Horn R G and Lawn B R 1990 *J. Mat. Res.* **5** 172–82
- Wan K T, Lathabai S and Lawn B R 1990 *J. European Ceram. Soc.* **6** 259–68
- Watanabe Y, Nakamura Y, Dickinson J T and Langford S C 1994 *J. Non-Cryst. Solids* **177** 9–25
- Weber N and Goldstein M 1964 *J Chem Phys* **41** 2898–901
- Wiederhorn S M 1967 *J. Am. Ceram. Soc.* **50** 407–14
- Wiederhorn S M 1969 *J. Am. Ceram. Soc.* **52** 99–105

- Wiederhorn S M and Bolz L H 1970 *J. Am. Ceram. Soc.* **53** 543–8
- Wiederhorn S M and Johnson H 1973 *J. Am. Ceram. Soc.* **56** 192–7
- Wiederhorn S M, Johnson H, Diness A M and Heuer A H 1974 *J. Am. Ceram. Soc.* **57** 336–41
- Wiederhorn S M, López-Cepero J M, Wallace J, Guin J P and Fett T 2007 *J. Non-Cryst. Solids* **353** 1582–91
- Wondraczek L, Ciccotti M, Dittmar A, Oelgardt C, Célarié F and Marlière C 2006 *J. Am. Ceram. Soc.* **89** 746–9
- Wright A C *Phys. Chem. Glasses* **49** 103–117
- Zarzycki J 1991 *Glasses and the Vitreous State* (Cambridge: Cambridge University Press)
- Zhu W, Porporati A A, Matsutani A, Lama N and Pezzotti G 2007 *J. Appl. Phys.* **101** 103531